Bioactive Materials 41 (2024) 46–60

Contents lists available at ScienceDirect

Bioactive Materials

journal homepage: www.keaipublishing.com/en/journals/bioactive-materials

Barnacle inspired strategy combined with solvent exchange for enhancing wet adhesion of hydrogels to promote seawater-immersed wound healing

Guiyuan Zhao [a], Aijia Zhang [a], Xiangyan Chen [a], Guangli Xiang [a], Tianze Jiang [a], Xia Zhao [a,b,*]

[a] Key Laboratory of Marine Drugs, Ministry of Education, Shandong Key Laboratory of Glycoscience and Glycotechnology, School of Medicine and Pharmacy, Ocean University of China, Qingdao, 266003, China
[b] Laboratory for Marine Drugs and Bioproducts of Qingdao National Laboratory for Marine Science and Technology, Qingdao, 266237, China

ARTICLE INFO

Keywords:
Barnacle
Solvent exchange
Hydrogel
Wet adhesion
Wound healing

ABSTRACT

Hydrogels are promising materials for wound protection, but in wet, or underwater environments, the hydration layer and swelling of hydrogels can seriously reduce adhesion and limit their application. In this study, inspired by the structural characteristics of strong barnacle wet adhesion and combined with solvent exchange, a robust wet adhesive hydrogel (CP-Gel) based on chitosan and 2-phenoxyethyl acrylate was obtained by breaking the hydration layer and resisting swelling. As a result, CP-Gel exhibited strong wet adhesion to various interfaces even underwater, adapted to joint movement and skin twisting, resisted sustained rushing water, and sealed damaged organs. More importantly, on-demand detachment and controllable adhesion were achieved by promoting swelling. In addition, CP-Gel with good biosafety significantly promotes seawater-immersed wound healing and is promising for use in water-contact wound care, organ sealing, and marine emergency rescue.

1. Introduction

Adhesive hydrogels have attracted considerable attention because of their wide range of applications, including wound dressings [1,2], surface glues [3–5], tissue sealants [6,7], motion monitoring, and wearable sensing technologies [8,9]. However, the biomedical applications of adhesive hydrogels in harsh wet or underwater environments faces great challenges. In particular, the workers at sea or underwater are vulnerable to the threat of open wounds, which are aggravated by hypertonic, alkaline, microbial-rich seawater, leading to high rates of disability and mortality [10,11]. Therefore, it is crucial to develop hydrogels that can protect wounds in wet and seawater environments. However, the hydrophilicity and high water content of hydrogels make it challenging to achieve strong wet adhesion [7]. More notably, once hydrogels are in contact with water or infiltrated by sweat or blood, the hydration layer formed between the interfaces severely reduces adhesion (Fig. 1). Swelling of hydrogels is another critical factor that affects their adhesion in a wet environment. Water absorption and swelling of hydrogels disrupt the functional bonds within the crosslinking network, allowing excess water to enter the network and resulting in a significant decrease in adhesion and mechanical properties [12–14]. Therefore, breaking the hydration layer and controlling appropriate swelling are key issues in achieving robust wet adhesion of hydrogels [15,16].

How to break the hydration layer between hydrogels and the applied surface? The key is to repel water molecules in the hydration layer [8]. Barnacles can achieve robust adhesion to ships, reefs, and even marine animals in seawater-surging environments by secreting a proteinaceous complex termed the "barnacle cement (BC)" [17]. BC mainly contains hydrophobic and cationic amino acids, which inspired us to break the hydration layer and increase the wet adhesion of hydrogels via strong hydrophobic and electrostatic interactions [18,19]. Moreover, Han et al. used Fe^{3+} to induce hydrophobic surfaces and successfully repelled water molecules from interfaces [20]. Wang et al. utilized the electrostatic interaction between imidazole and carboxyl groups to achieve strong wet adhesion of hydrogels [12]. Previous studies have demonstrated that it is feasible to break the hydration layer through hydrophobic and electrostatic interactions to enhance the wet adhesion of hydrogels. In addition, polysaccharides in BC, especially chitin, play an important role in adhesion function [21–23]. However, most barnacle-inspired studies are based on the protein structure in BC [7,24,25], ignoring the important roles of chitin. Therefore, designing adhesive materials based on the function of chitin in BC is a novel and

Peer review under responsibility of KeAi Communications Co., Ltd.
* Corresponding author. Key Laboratory of Marine Drugs, Ministry of Education, School of Medicine and Pharmacy, Ocean University of China, Qingdao, 266003, China.
E-mail address: zhaoxia@ouc.edu.cn (X. Zhao).

https://doi.org/10.1016/j.bioactmat.2024.07.011
Received 16 January 2024; Received in revised form 25 June 2024; Accepted 5 July 2024

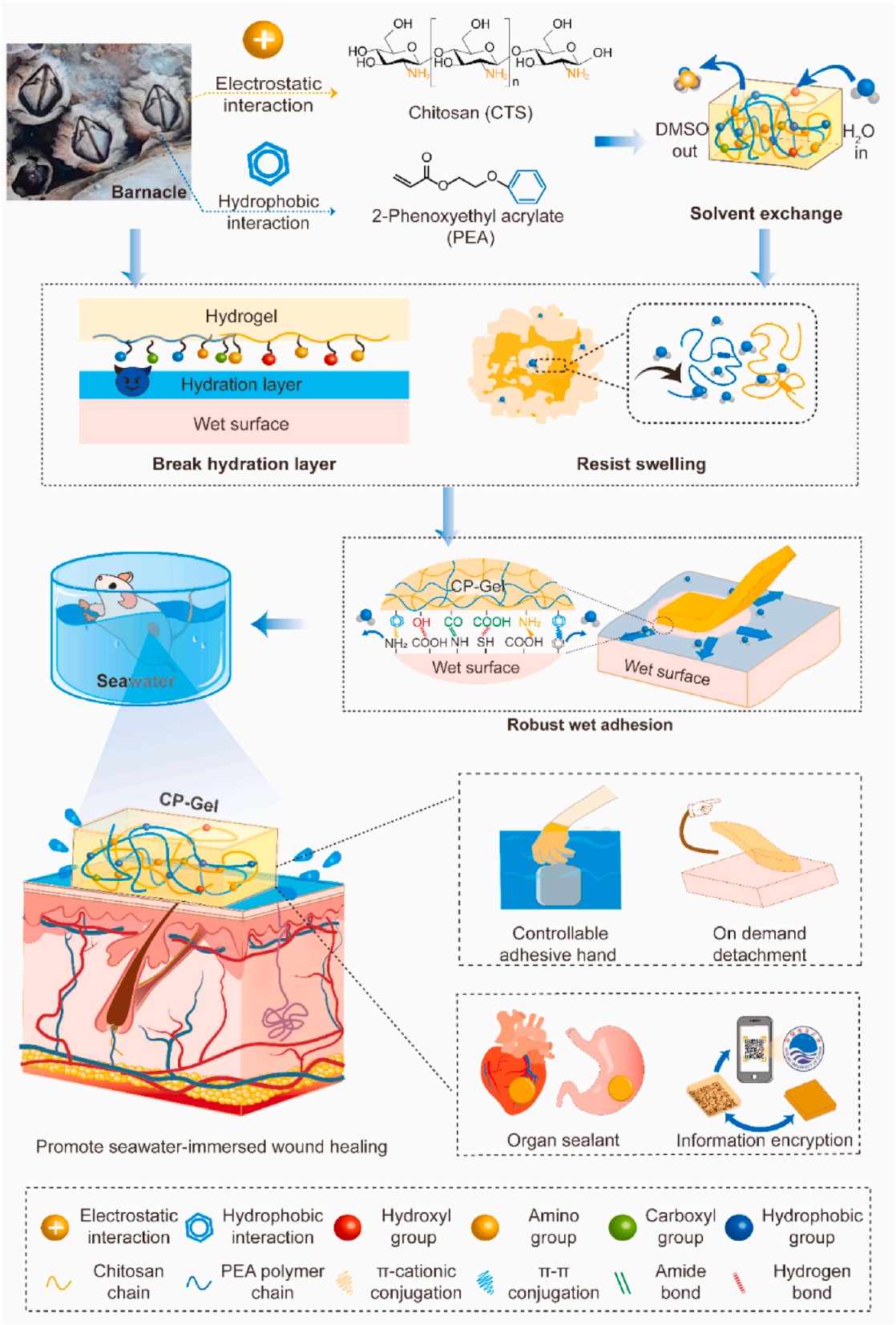

Fig. 1. Barnacle inspired strategy combined with solvent exchange to enhance wet adhesion of hydrogels for seawater-immersed wound healing. CTS and PEA were used to mimic the structural characteristics of BC and remove the detrimental effect of the hydration layer on adhesion, and solvent exchange strategies were used to prepare CP-Gel to resist swelling. CP-Gel was used for promoting seawater-immersed wound healing, controllable wet adhesive hand, organ sealant, and information encryption.

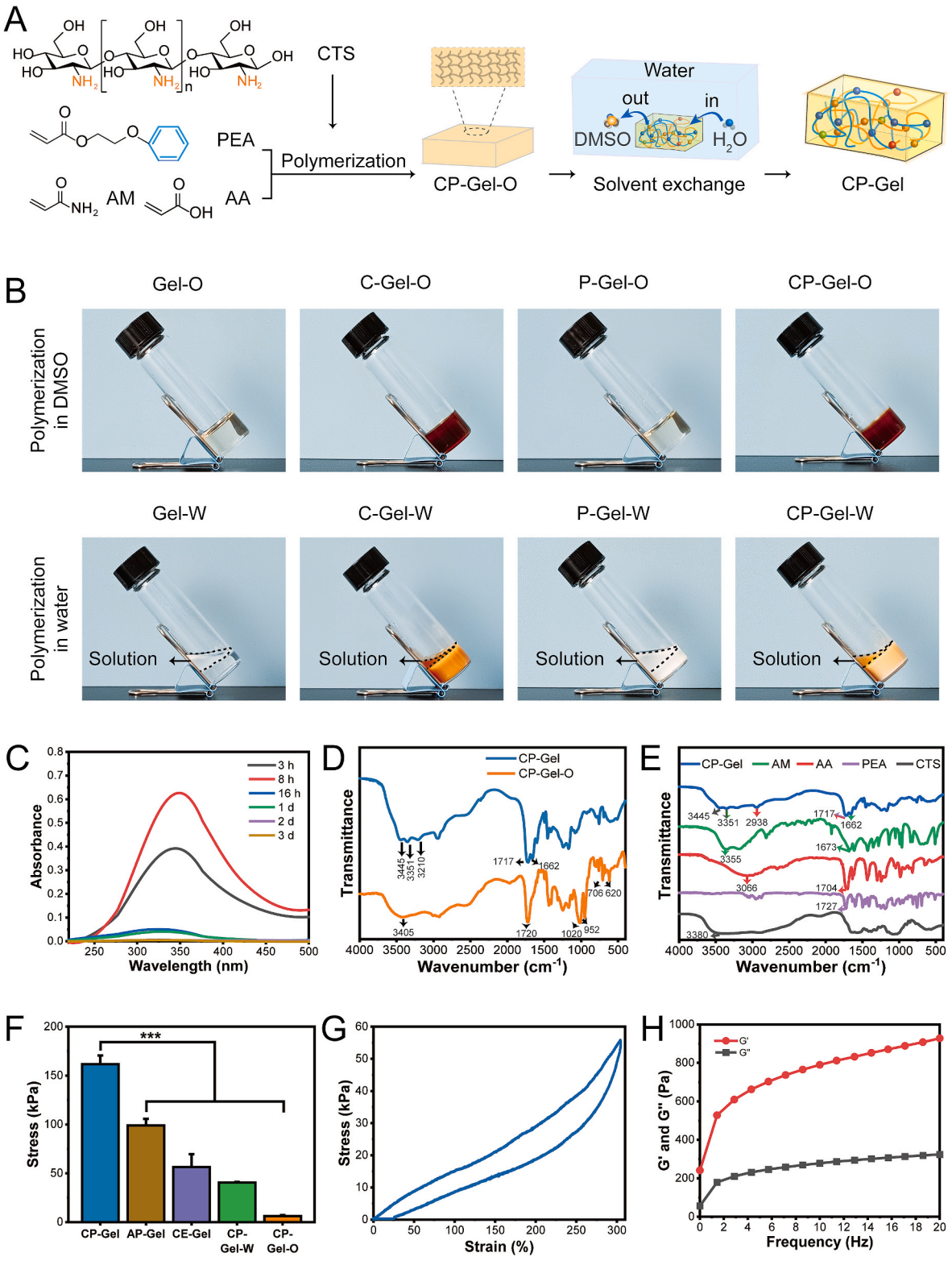

Fig. 2. Preparation and characterization of hydrogels. (A) Schematic of CP-Gel fabrication. CTS and PEA are polymerized into an organogel (CP-Gel-O) by free radical polymerization reaction with AA and AM in a good solvent of DMSO. Then, CP-Gel-O is placed in water for solvent exchange to prepare CP-Gel. (B) Gel photographs polymerized in DMSO or water. (C) UV absorption of CP-Gel immersing solution by solvent exchange at different time points. (D) Comparison of infrared spectra of CP-Gel and CP-Gel-O in the range of 4000-400 cm^{-1}. (E) Comparison of infrared spectra of CP-Gel and its component including CTS, PEA, AA and AM in the range of 4000-400 cm^{-1}. (F) Tensile strength of CP-Gel and control hydrogels. (G) Stress-strain curve of CP-Gel stretching to 300 % in one cycle. (H) Rheological frequency scan results of CP-Gel. Data are expressed as mean ± SD (n = 5).

promising strategy.

How to control the appropriate swelling of hydrogels? It has been shown that a homogeneous and dense network of hydrogels is an important factor affecting swelling, and the double-network structure shows better anti-swelling ability [26–29]. Solvent exchange is a promising strategy to construct anti-swelling double-network hydrogels [13,30]. In other words, after homogenizing the hydrogel network in a good solvent, a high cross-linking density network can be constructed by solvent exchange [12,31,32], which can effectively resist water absorption and swelling to improve the wet adhesion of hydrogels.

Chitosan (CTS) is a natural cationic polysaccharide derived from chitin that has excellent safety, hemostatic, and wound healing properties [33–35]. 2-Phenoxyethyl acrylate (PEA) is a compound containing a benzene ring, which can affect the hydrogen bonds between water molecules to make the hydrogel water-repellent and break the hydration layer [31]. Therefore, inspired by the robust adhesion of marine barnacles, we selected CTS to mimic electrostatic interactions and chitin skeleton structures and PEA to mimic hydrophobic interactions in BC

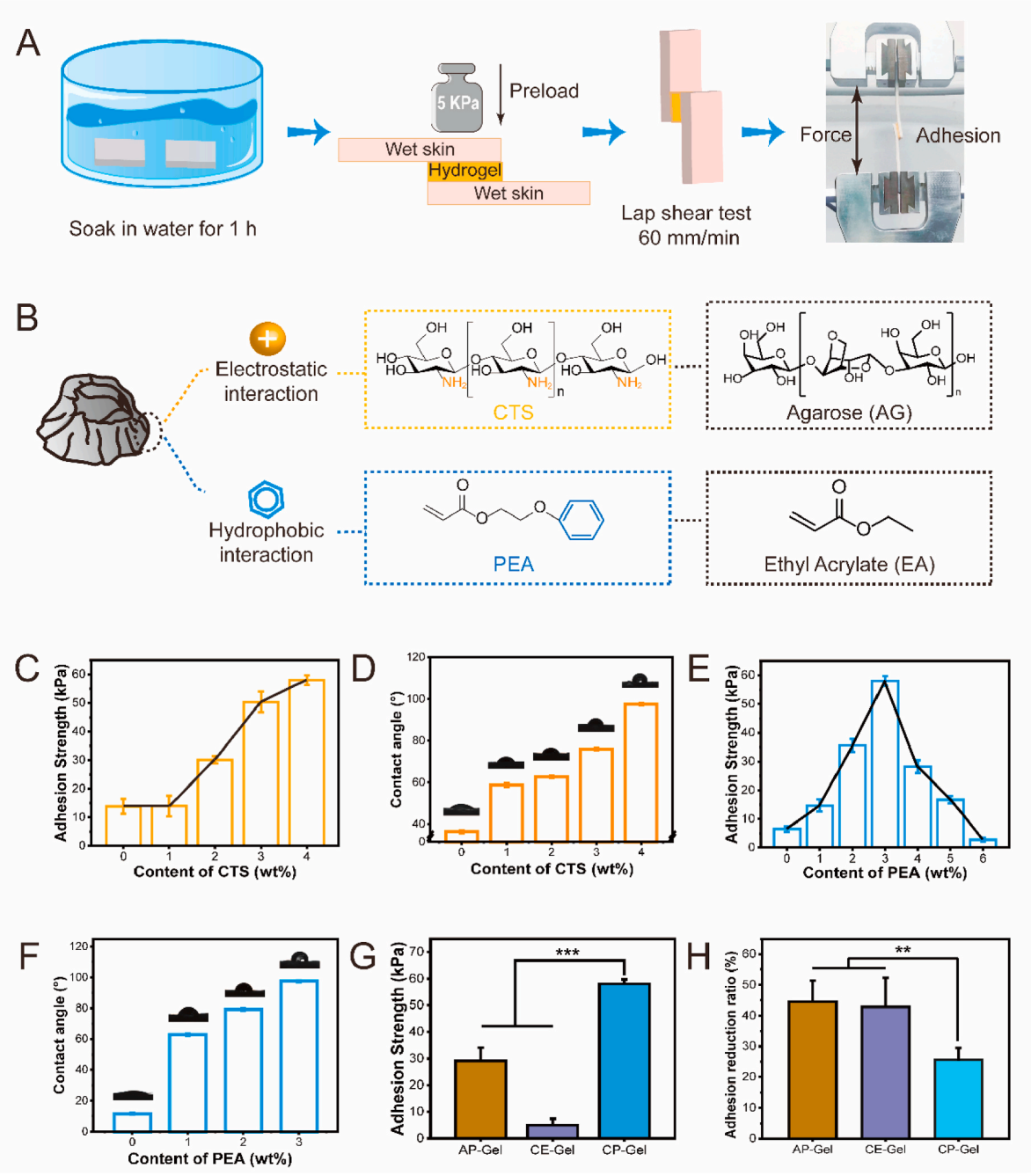

Fig. 3. CTS and PEA achieve wet adhesion by breaking hydration layer. (A) Schematic of lap-shear test. After soaking fresh pig skin in water for 1 h, hydrogel is adhered between two pieces of pig skin, and then preloading strength of 5 kPa is applied for 30 s. The pig skin with adhered hydrogels is fixed to the shear mold of the universal testing machine and tested at a speed of 60 mm min^{-1}. (B) Molecular structure of control hydrogels. AP-Gel is prepared by replacing CTS with AG without charge group, and CE-Gel is prepared by replacing PEA with EA without hydrophobic aromatic rings. (C) Effects of CTS content on wet adhesion strength. (D) Contact angles of hydrogels with different CTS contents. (E) Effects of PEA content on wet adhesion strength. (F) Contact angles of hydrogels with different PEA contents. (G) Comparison of adhesion strength of CP-Gel, AP-Gel, and CE-Gel. (H) Effect of hydration layer on adhesion of CP-Gel, AP-Gel, and CE-Gel. Data are expressed as mean ± SD, sample number: n = 3 in (D, F) and n = 5 in (C, E, G, H), ***$P < 0.001$, **$P < 0.01$.

and to break the hydration layer on wet adhesion, respectively.

To enhance the anti-swelling properties of hydrogels, CTS and PEA were formed into a CTS-PEA hydrogel (CP-Gel) by solvent exchange between dimethyl sulfoxide (DMSO) and water. We hypothesized that the barnacle-inspired strategy combined with solvent exchange could enhance the wet adhesion of hydrogels by breaking the hydration layer and resisting swelling. Furthermore, the ability of organ sealant, seawater-immersed wound healing, on-demand detachment, controllable adhesion, and information encryption were also used to evaluate the potential application of CP-Gel. This strategy provides a novel idea for the development of strong wet adhesive hydrogels and exhibits a wide range of application prospects (Fig. 1).

2. Materials and methods

2.1. Preparation of CP-Gel

CTS and PEA were selected to build covalent network hydrogels by mimicking the structural features of BC. DMSO (1.2 mL) was added to CTS (52.8 mg, 4 wt% of DMSO) and stirred until completely dissolved. Then PEA (39.6 mg, 3 wt% of DMSO), matrix acrylic acid (AA, 132.0 mg, 10 wt% of DMSO), acrylamide (AM, 66.0 mg, 5 wt% of DMSO), N, N - methylenebisacrylamide (MBA, 0.5 mg, 0.2 wt% of total weight of monomer compounds), and ammonium persulfate (APS, 7.1 mg, 3 wt% of total weight of monomer compounds) were added, and CTS-PEA organogel (C-Gel-O) was prepared by polymerization at 50 °C for 12 h. Then, CP-Gel-O was placed in water for 3 d, and the water was changed every 8 h to fully remove DMSO and unreacted cross-linked monomer to obtain CP-Gel (stored at 4 °C).

2.2. Preparation of control hydrogels

The AA-AM organogel without CTS and PEA (Gel-O), CTS organogel (C-Gel-O), PEA organogel (P-Gel-O), agarose (AG)-PEA organogel (AP-Gel-O), and CTS-ethyl acrylate (EA) organogel (CE-Gel-O) were prepared in DMSO at 50 °C for 12 h. Their compositions and characteristics are listed in Table S1. Then, the AA hydrogel (Gel), CTS hydrogel (C-Gel), PEA hydrogel (P-Gel), AG-PEA hydrogel (AP-Gel), and CTS-EA hydrogel (CE-Gel) were prepared by solvent exchange with water for 3 d, and the water was changed every 8 h.

AA-AM, CTS, PEA, CTS-PEA hydrogel without solvent exchange (Gel-W, C-Gel-W, P-Gel-W, CP-Gel-W) were prepared by dispersing identical compositions in water as those of the Gel, C-Gel, P-Gel, and CP-Gel, respectively, followed by polymerization at 50 °C for 12 h.

2.3. Characterization of CP-Gel and control hydrogels

Detailed characterizations of CP-Gel and control hydrogels are provided in the Supplementary Materials.

3. Results and discussion

3.1. Synthesis and characterization of hydrogels

CP-Gel was synthesized by the polymerization of CTS and PEA combined with solvent exchange (Fig. 2A). To investigate the effects of CTS and PEA on the properties of the hydrogels, hydrogels without PEA (C-Gel), CTS (P-Gel), and CTS and PEA (Gel) were prepared using the same method. To reduce the adverse effects of swelling on the wet adhesion of hydrogels, we used a solvent exchange strategy of DMSO and water to construct homogeneous hydrogels with covalent-physical double cross-linked networks. As shown in Fig. 2B and Fig. S1, all organogels polymerized in DMSO were transparent and intact gels, whereas Gel-W, C-Gel-W, P-Gel-W, and CP-Gel-W polymerized in water were incompletely cross-linked turbid solutions. This indicates that the first step of solvent exchange, which involves polymerization in a good solvent of DMSO, is favorable for the preparation of covalent networks [36].

The solution was monitored by UV spectrophotometry during solvent exchange. As shown in Fig. 2C, the solution no longer showed significant UV absorption after 2 d, indicating that the DMSO and unreacted cross-linked monomers were completely removed. In the IR spectra of CP-Gel (Fig. 2D), the stretching vibrational peak of S=O at 1020 cm^{-1}, bending vibrational peak of C-H at 952 cm^{-1}, and stretching vibrational peaks of C-S-C at 706 cm^{-1} and 620 cm^{-1} of DMSO disappeared, which also demonstrated the effective removal of DMSO [37]. After solvent exchange, the absorption peaks of OH at 3380 cm^{-1} for CTS, NH_2, C=O at 3355 cm^{-1} and 1673 cm^{-1} for AM, OH at 3066 cm^{-1}, C=O at 1704 cm^{-1} for AA, and C=O at 1727 cm^{-1} for AA shifted to lower wavelengths (Fig. 2E and Fig. S2). These results indicate that intermolecular hydrogen bonds between polymers were established [30,38], suggesting that a dynamic physical cross-linking network was constructed based on a covalent network by solvent exchange [39].

Next, we verified whether the double network constructed by solvent exchange enhanced the mechanical properties of the hydrogels. CP-Gel-O broke off when stretched to 3 times its length, while CP-Gel could be stretched to 6 times its length and resisted a tensile strength of 161.67 ± 8.99 kPa (Fig. 2F and Fig. S3). In a loading and unloading cycle with a maximum strain of 300 %, CP-Gel exhibited an obvious hysteresis loop (Fig. 2G) with a maximum stress of 54.79 kPa, indicating that CP-Gel had a strong energy dissipation capacity [12]. In addition, the energy storage modulus (G′) of CP-Gel was consistently higher than the loss modulus (G′′) in the frequency range of 0.1–20 Hz (Fig. 2H), indicating that the hydrogel has good structural stability. Collectively, CTS and PEA were selected to form covalent and physical double-network structures via solvent exchange. CP-Gel exhibited good tensile properties, energy dissipation properties, and structural stability, which are favorable for wet adhesion and resistance to external force damage [40,41].

3.2. Effects of CTS and PEA on hydration layer

Adhesive interfaces (such as the skin) tend to form hydration layers in wet environments because of their rich functional groups [42], which can block the interaction between the hydrogels and functional groups, thereby seriously affecting their adhesion. To investigate the repulsion between CTS and PEA in the hydration layer, we evaluated the adhesion strength of the hydrogels to wet pigskins soaked in water using lap-shear experiments (Fig. 3A). As shown in Fig. 3C and D, the adhesion strength and contact angle of the hydrogels were positively correlated with the CTS content, which was attributed to the electrostatic interactions of the CTS amino groups enhancing the repulsion of water. In addition, the barnacle chitin-like structure of CTS may play a favorable role in enhancing hydrogel cohesion and wet adhesion. However, it was difficult to form hydrogels when the content of CTS was higher than 4 wt%, mainly because a high CTS content hindered the free-radical polymerization of the monomers [43]. As shown in Fig. 3E, the adhesion strength of the hydrogels reached a maximum at a PEA content of 3 wt% when the CTS content was fixed at 4 wt%. This could be because the increase in PEA content promoted the repulsion of hydrophobic aromatic rings to water molecules (Fig. 3F) [1,39,44]. To prove this, the hydrated layer was visualized on the surface of the pigskin using a methylene blue solution. As shown in Fig. S4, CP-Gel (containing PEA) showed a thinner hydration layer than the surrounding area, whereas C-Gel (without PEA) still showed a thick hydration layer, suggesting that the addition of PEA indeed helps weaken the hydration layer. However, excessive surface aggregation of hydrophobic groups is unfavorable for the adhesion of hydrogels when the PEA content is too high [45]. These results indicate that the optimum contents of CTS and PEA for CP-Gel were 4 wt% and 3 wt%, respectively.

To further verify the effects of cationic polysaccharides and hydrophobic aromatic compounds on the hydration layer (Fig. 3B), we

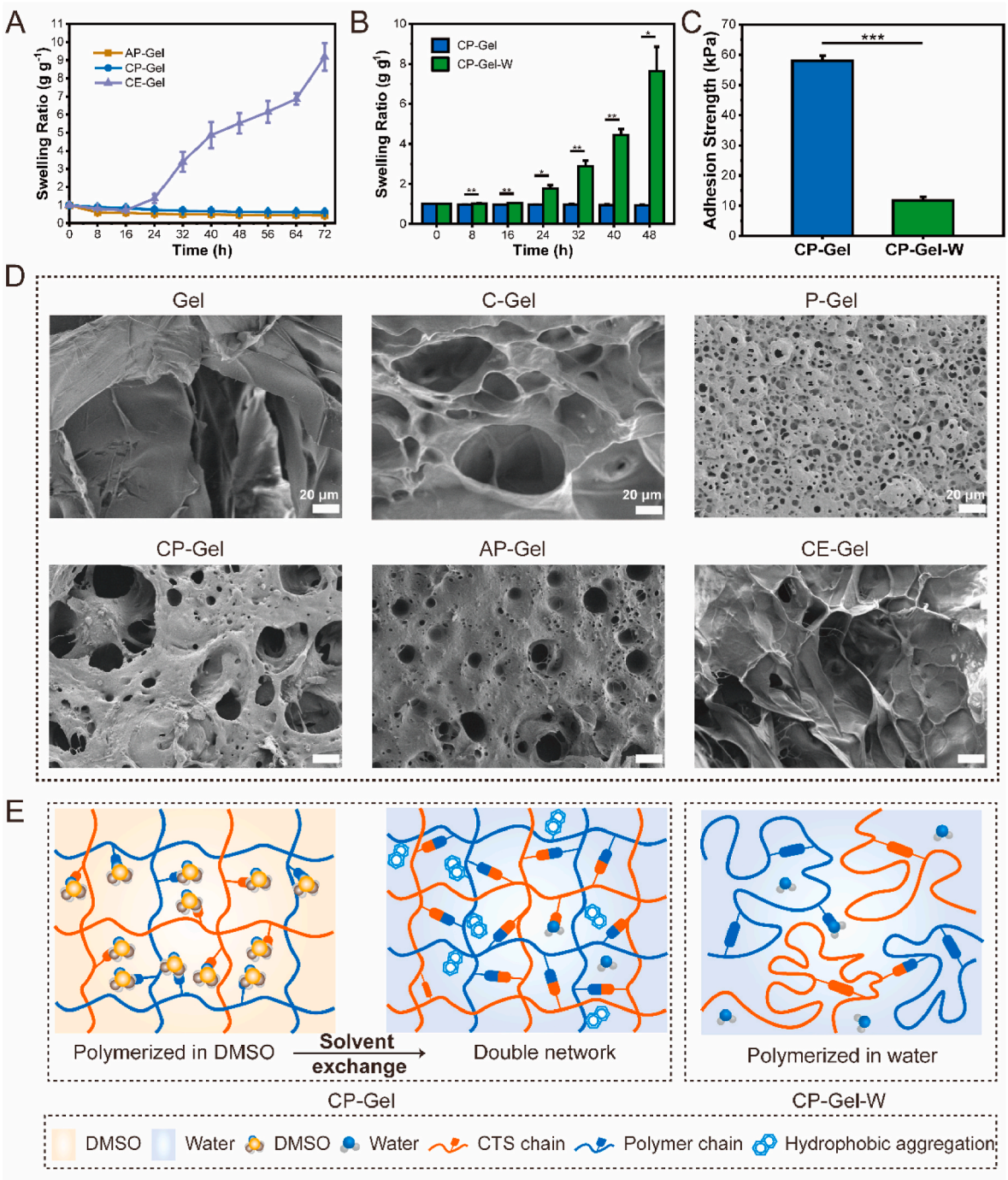

Fig. 4. Swelling and property changes of gel during solvent exchange. (A) Comparation of swelling rates of AP-Gel, CE-Gel and CP-Gel at different time points. (B) Comparison of swelling rate between CP-Gel and CP-Gel-W within 48 h. (C) Comparison of adhesion strength of CP-Gel and CP-Gel-W. (D) SEM images of Gel, C-Gel, P-Gel, CP-Gel, AP-Gel, and CE-Gel. Scale bar = 20 μm. (E) Schematic of a homogeneous network structure formed by solvent exchange and the structure of hydrogels polymerized directly in water. Data are expressed as mean ± SD, sample number: n = 3 in (A–B) and n = 5 in (C). ***$P < 0.001$, **$P < 0.01$, *$P < 0.05$.

replaced CTS with uncharged AG to prepare AP-Gel, and replaced PEA with aromatic ring-free EA to synthesize CE-Gel. As shown in Fig. 3G, AP-Gel exhibited an adhesion strength of 29.12 ± 4.96 kPa, which was significantly lower than that of CP-Gel (58.04 ± 1.67 kPa), while CE-Gel only exhibited a lower adhesion strength of 5.03 ± 2.33 kPa. In addition, we evaluated the effect of the hydration layer on adhesion strength based on the difference between CP-Gel and control hydrogels on dry and wet skin. As shown in Fig. 3H, the adhesion strength was reduced by more than 40 % under the influence of the hydration layer, which was significantly higher than the 25.7 ± 3.8 % of CP-Gel. These results further indicate that CTS and PEA play a crucial role in breaking the hydration layer to achieve a strong wet adhesion of the hydrogels.

3.3. *Effect of solvent exchange strategy on swelling*

Swelling of hydrogels can lead to the disruption of functional bonds within the cross-linked network, thereby decreasing their adhesion and mechanical properties [13]. Moreover, highly swollen hydrogels are prone to the physical compression of bioadhesive interfaces such as the skin, causing pain and secondary injuries [46]. Therefore, maintaining

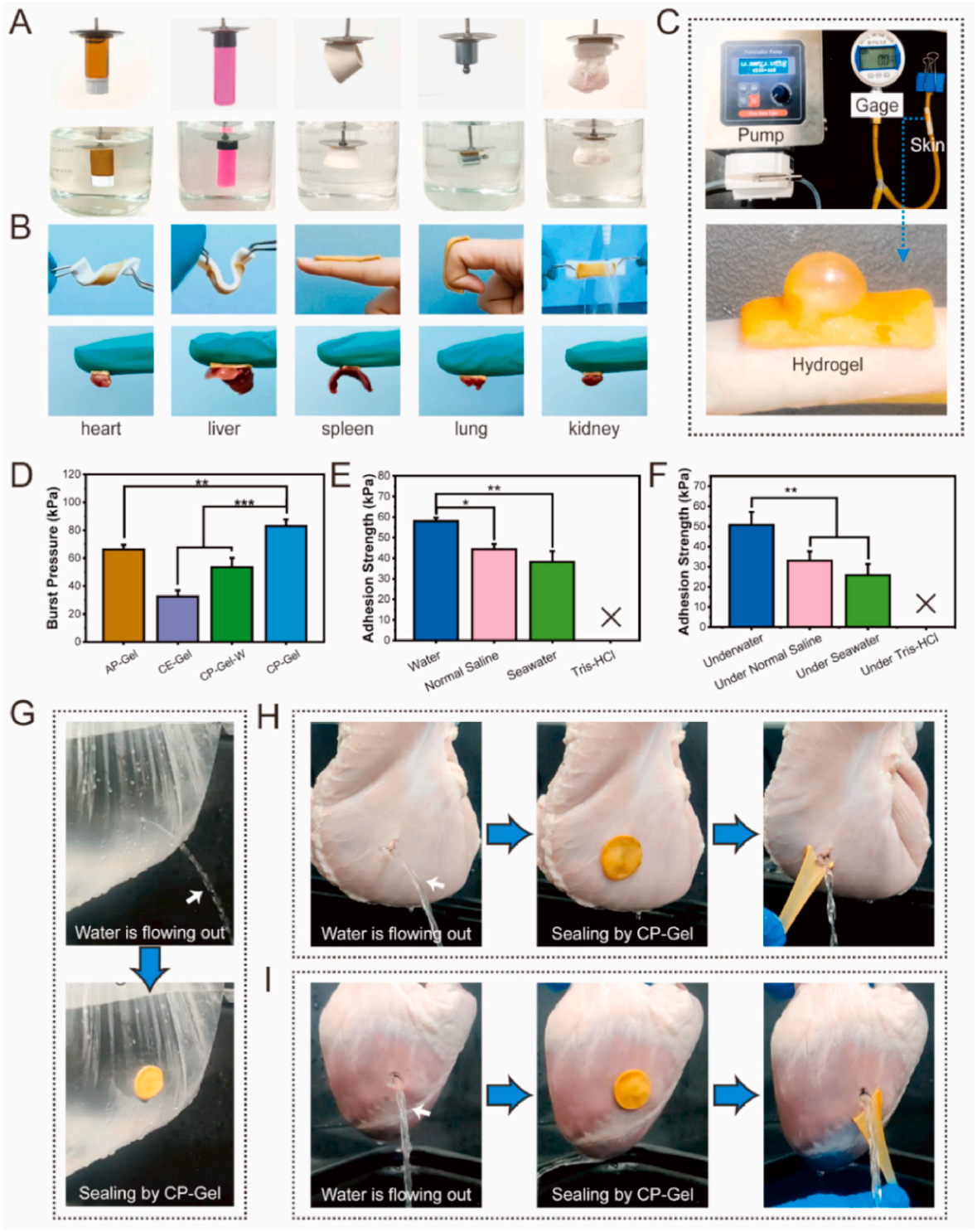

Fig. 5. Adhesion properties of CP-Gel. (A) CP-Gel can adhere and lift glass, plastic, rubber, metal, and pig tissue underwater. (B) CP-Gel adapts the movement of the skin tissue, resists water washing, and adheres to skin tissue and organs. (C) Experimental device for bursting pressure. (D) Burst pressure of different hydrogels. Adhesion strength of CP-Gel to pig skins soaked in (E) or under (F) water, saline, seawater, and Tris-HCl buffers. (G) CP-Gel adheres to a plastic bag and blocks the running water. CP-Gel seals leaking pig stomach (H) and heart (I), and when CP-Gel is removed the sealed organ gaps leak again. Data are expressed as mean ± SD, sample number: n = 3 in (D) and n = 5 in (E–F). $^{***}P < 0.001$, $^{**}P < 0.01$, $^{*}P < 0.05$.

swelling stability is essential for the wet adhesion of hydrogels.

First, we explored the swelling behavior of CP-Gel during solvent exchange. As shown in Fig. 4A and Fig. S5, the swelling rates of Gel, C-Gel, and CE-Gel without PEA reached 12.60 ± 0.36 g g^{-1}, 17.11 ± 0.77 g g^{-1}, and 9.18 ± 0.75 g g^{-1}, respectively. In addition, scanning electron microscope (SEM) images showed that P-Gel, AP-Gel, and CP-Gel had surfaces with aggregated hydrophobic phases and denser network structures after solvent exchange, whereas the hydrogels without PEA had large pores and loose networks (Fig. 4D). These results suggest that solvent exchange causes hydrophobic PEA to aggregate on the hydrogel surface, thereby resisting the intrusion of water molecules into the hydrogel backbone [45,47]. However, a high swelling resistance can

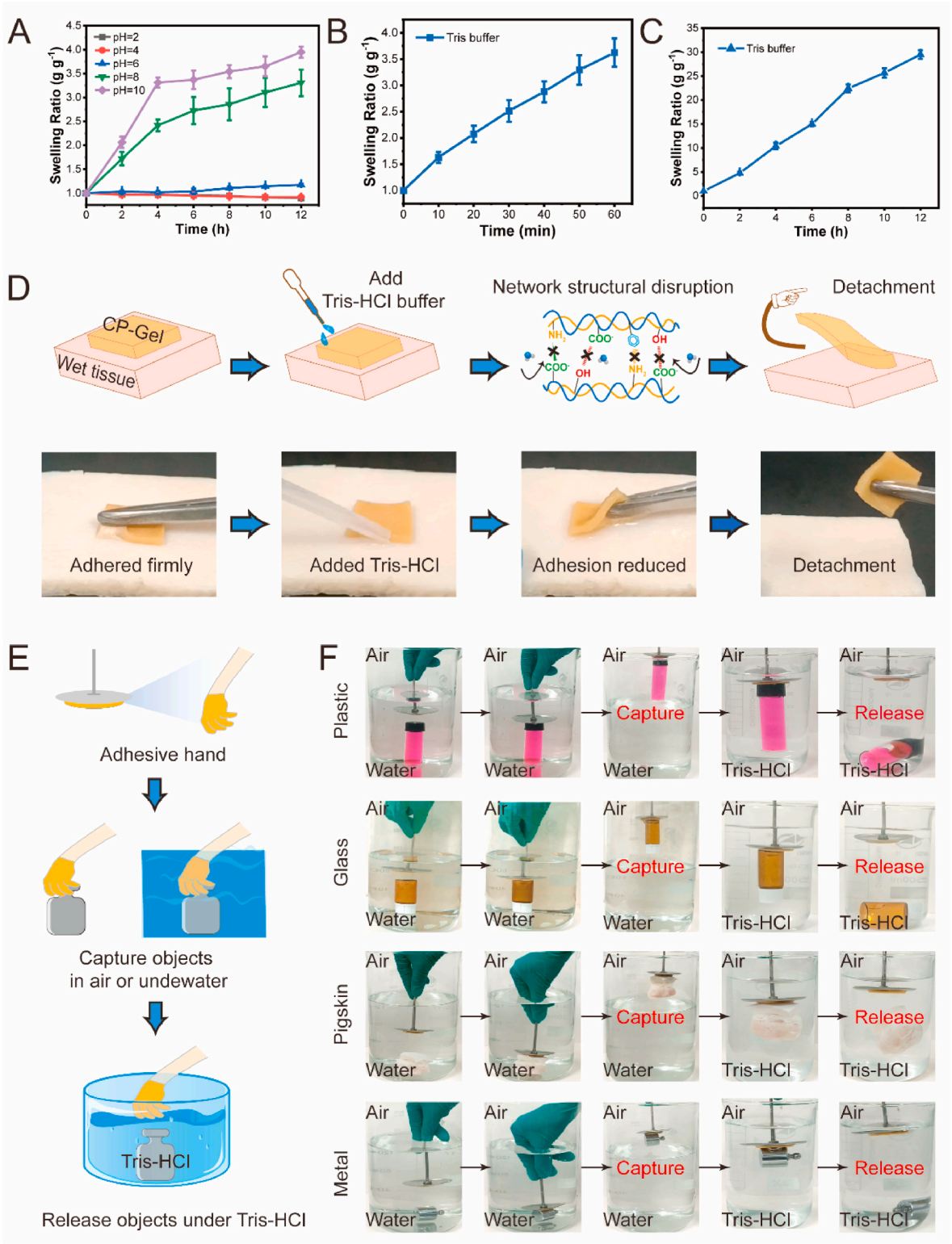

Fig. 6. Controllable adhesion of CP-Gel. Swelling ratio of CP-Gel in different pH solutions in 12 h (A), and Tris-HCl buffer solutions in 60 min (B) and 12 h (C). (D) On-demand detachment of CP-Gel with Tris-HCl buffer solution (0.15 mol L^{-1}, pH 8). (E) Diagram of a controllable hydrogel adhesive hand. (F) Controlled capture and release of plastic, glass, pigskin and metal using a hydrogel adhesive hand. Data are expressed as mean ± SD (n = 3).

lead to excessive shrinkage and aggregation of polymer chains, resulting in decreased water content, flexibility, and extensibility of hydrogels [14,48]. For example, although P-Gel (Fig. S6) and AP-Gel (Fig. S7) had stronger swelling resistance than that of CP-Gel, they exhibited severe water loss, smaller pore sizes, and more aggregated structures (Fig. 4D), which was unfavorable for wet adhesion.

To further investigate the effect of solvent exchange on the hydrogels, we evaluated the swelling and adhesion properties of CP-Gel synthesized by solvent exchange and CP-Gel-W directly polymerized in water. The results showed that CP-Gel exhibited lower swelling rates at

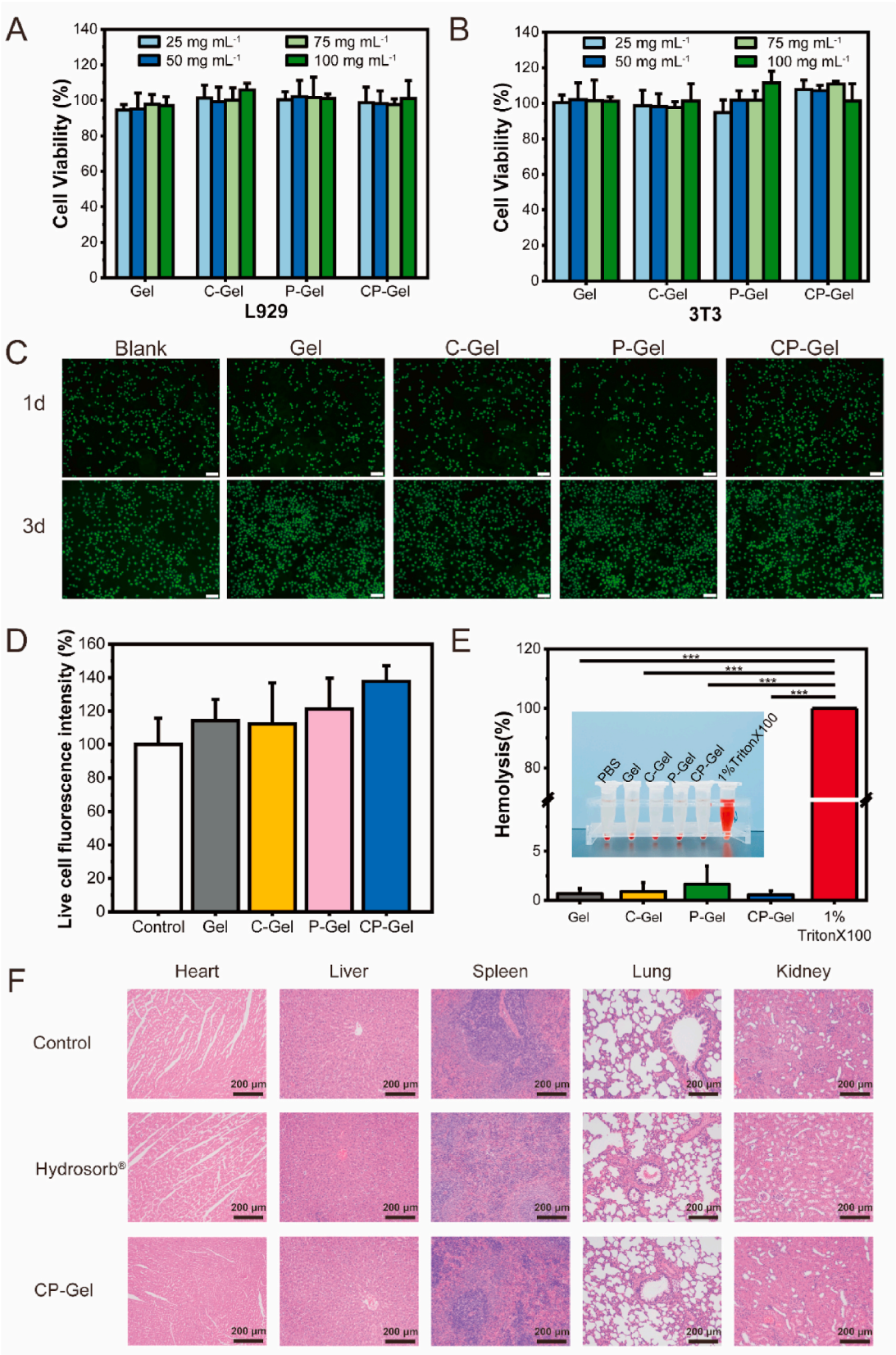

Fig. 7. Biocompatibility of hydrogels. Cell viabilities of L929 cells (A) and 3T3 cells (B). (C) Live-dead cell staining results of L929 cells at 1 d and 3 d. Scale bar: 100 μm. (D) Fluorescence quantification of L929 living cells treated with different hydrogels for 3 d. (E) Hemolysis of erythrocytes after co-incubation with Gel, C-Gel, P-Gel, and CP-Gel. (F) H&E staining of various organs of rats treated with hydrogels. Data are expressed as mean ± SD (n = 3). ***$P < 0.001$.

48 h (Fig. 4B), indicating that solvent exchange is beneficial for the structural stability of hydrogels [30,49]. As shown in Fig. S8, the contact angle of CP-Gel was 97.58 ± 0.56°, which was higher than that of CP-Gel-W at 82.84 ± 0.59°. The contact angle results prove that CP-Gel has better water repellency after solvent exchange, which is beneficial for resisting the swelling triggered by the intrusion of water molecules and maintaining the stable structure of the hydrogel [44]. In addition, when water is used as a solvent, the polymer chains are curled and twisted, and are unable to form a homogeneous covalent network owing to the strong interaction between the polymer chains [30,32]. In contrast, DMSO can form chain-solvent hydrogen bonds with the gel polymer chains to promote covalent network homogeneity (Fig. 4E), which contributes to CP-Gel resisting swelling better than CP-Gel-W [47,50]. As shown in Fig. 4C, the adhesion behavior of CP-Gel (58.04 ± 1.67 kPa) was significantly better than that of CP-Gel-W (11.76 ± 1.18 kPa). These results indicate that CP-Gel has a more stable structure and anti-swelling properties after solvent exchange, which is beneficial for improving its wet adhesion.

Interestingly, the solvent exchange process is accompanied by the aggregation and stretching of polymer chains in the gel network, leading to a solvent-induced shift in gel transparency, which is promising for information encryption and decryption [51]. As shown in Figs. S9–10, CP-Gel-O is transparent in DMSO and can clearly present a quick response (QR) code with the embedded information. When CP-Gel-O was placed in water for 15 min, the water molecules induced the aggregation of polymers, leading to gradual opacity of the gel; thus, the QR code information was encrypted. In turn, DMSO rapidly transforms the hydrogel from opaque to transparent, thus decrypting the hidden information.

3.4. Wet and underwater adhesion of CP-Gel

CP-Gel exhibits good adhesion to different surfaces under various wet conditions. As shown in Fig. 5A, CP-Gel can adhere to and lift glass, plastic, rubber, metal, and pig tissues in air and underwater. The good adhesion and tensile properties of CP-Gel enable it to adapt to joint movement (Fig. 5B and Movie S1), and it can firmly adhere even when the skin tissues are twisted and bent (Movie S2), which is expected to be used as a motion-sensing material. Movie S3 shows that CP-Gel adhered firmly to the skin tissue and resisted sustained water rushing. In addition, CP-Gel can firmly adhere to skin tissues and various organs and is expected to be used in surgical procedures.

Supplementary video related to this article can be found at https://doi.org/10.1016/j.bioactmat.2024.07.011

Adhesives for *in vivo* applications are often subjected to adhesion and mechanical property challenges caused by abdominal or thoracic pressures. To evaluate the potential of CP-Gel for *in vivo* applications, we measured the maximum pressure the hydrogel could withstand using burst pressure experiments (Fig. 5) [11]. CP-Gel can withstand a burst pressure of 83.0 ± 4.6 kPa, which is significantly higher than those of AP-Gel and CE-Gel without barnacle inspired strategy and CP-Gel-W without solvent exchange (Fig. 5D).

We also evaluated the adhesion of the hydrogels in different environments (Fig. 5E). With only 5-kPa preloading, CP-Gel presented an adhesion strength of 58.04 ± 1.67 kPa to wet pig skin, which is superior to the hydrogels based on schiff base reaction and catechols, and 5 times stronger than that of commercially available bioadhesives [20,52–54]. CP-Gel also exhibited good adhesion to saline and seawater-soaked skin with the adhesion strength of 44.34 ± 2.58 kPa and 38.14 ± 5.27 kPa, respectively. Additionally, CP-Gel exhibited robust adhesion to water, saline, and seawater (Fig. 5F and Fig. S11), suggesting their potential for wound protection during underwater emergency rescue.

In addition, the excellent wet adhesion properties indicate the potential of CP-Gel for sealing leakage. CP-Gel can adhere to a plastic bag that is leaking water, sealing the gap and stopping the flow of water (Fig. 5G and Movie S4), indicating that CP-Gel can seal the leakage of hydrophobic materials. A leakage 6 mm in diameter was cut into the stomach (Fig. 5H and Movie S5) and heart (Fig. 5I), and CP-Gel effectively sealed the leakage and stopped the water flow in less than 5 s. The rapid sealing capability of CP-Gel is promising for clinical use in repairing internal wounds such as ulcers and penetrating injuries [55,56].

Supplementary video related to this article can be found at https://doi.org/10.1016/j.bioactmat.2024.07.011

3.5. On-demand detachment of CP-Gel and controllable hydrogel adhesive hand

Non-covalent bonding is an important factor for CP-Gel to maintain a stable cross-linked structure and achieve wet adhesion. Changes in non-covalent swelling in different environments can be utilized to regulate the structure and adhesive properties of hydrogels. The swelling behavior of CP-Gel immersed in different solutions was evaluated. We found that CP-Gel was relatively stable in low pH environments, but the swelling rate significantly increased at pH 8 and pH 10 after 12-h immersion, which were 3.31 ± 0.28 g g^{-1} and 3.95 ± 0.12 g g^{-1}, respectively (Fig. 6A). This is mainly due to the dissociation of the rich carboxyl groups in the hydrogels in alkaline environments, which can bind more water molecules to break hydrogen bonds and electrostatic interactions [12].

In addition, the swelling rate of CP-Gel in tris (hydroxymethyl) aminomethane hydrochloride (Tris-HCl) was positively correlated with time (Fig. 6B–C), reaching 1.63 ± 0.10 g g^{-1} at 10 min and 29.51 ± 0.90 g g^{-1} at 12 h. This may be because Tris-HCl interacts with the charged groups of hydrogels, thus weakening the electrostatic interactions in the network [48,57]. The swelling of CP-Gel in the Tris-HCl buffer solution can be used to control the adhesive behavior. As shown in Fig. 5E–F, CP-Gel showed no adhesion to alkaline Tris-HCl. This significant reduction in CP-Gel adhesion in specific solutions offers bright prospects for the design of hydrogels with controllable adhesion and on-demand detachment. Fig. 6D and Movie S6 show the on-demand detachment of the hydrogels with the Tris-HCl buffer solution. The hydrogel adhered firmly to pig skin and was difficult to peel off. However, when a 0.15 mol L^{-1} Tris-HCl buffer solution was dropped onto the hydrogel-adhesion interface, the hydrogel was completely detached without residue. The results indicate that CP-Gel can minimize the difficulty of wound debridement, reduce pain during dressing changes, and avoid secondary injury in the biomedical field through an alkaline buffer solution [58].

Supplementary video related to this article can be found at https://doi.org/10.1016/j.bioactmat.2024.07.011

Furthermore, a CP-Gel with extended arms was designed as a controllable hydrogel hand (Fig. 6E) that could capture objects such as plastic, glass, pigskin, rubber, and metal in air or underwater environments because of its strong adhesion (Fig. 6F and Movie S7-8). By contrast, when the captured object was placed in Tris-HCl, the hydrogel adhesive hand released the object on demand. This controlled capture and release provides the possibility for surgery, wearable electronic devices, grippers, and dynamic accessories [59].

Supplementary video related to this article can be found at https://doi.org/10.1016/j.bioactmat.2024.07.011

3.6. Biocompatibility of CP-Gel

Good biocompatibility is the basis for the application of hydrogels in biomedicine. Cytocompatibility of the hydrogels was examined using a cell viability assay (CCK-8). As shown in Fig. 7A–B, the survival ratios of L929 and 3T3 cells in all hydrogel extracts were above 90 %, indicating that the hydrogels were safe for cells. The cytocompatibility of the hydrogels was further evaluated by live-dead cell staining. As shown in Fig. 7C and Fig. S12, L929 cells cultured in the hydrogel-immersed solution had a normal pike-shaped morphology and exhibited a

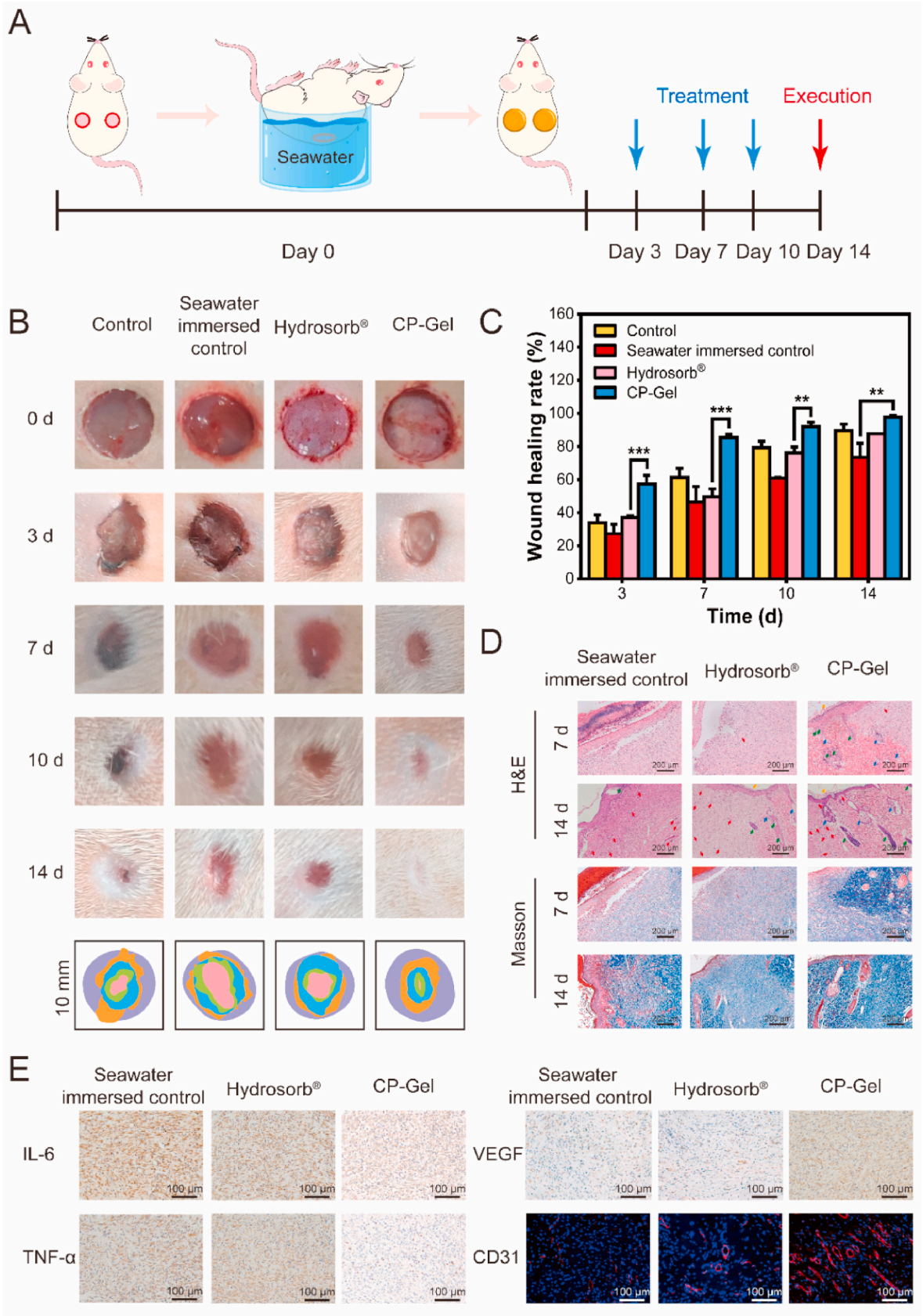

Fig. 8. Wound healing in seawater-immersed model. (A) Schematic of the experimental seawater-immersed whole-layer wound model in rats. (B) Wound images at 0, 3, 7, 10, and 14 d in different treatment groups. (C) Wound healing rate at 0, 3, 7, 10, and 14 d in different treatment groups. (D) H&E and Masson staining images of wounds at 7 and 14 d in different treatment groups. Red arrows: neovascularization; blue arrows: neovascular sebaceous glands; green arrows: neovascular hair follicles; yellow arrows: neovascular epithelium. In Masson staining images, collagen is shown in blue. (E) Immunohistochemistry of IL-6, TNF-α, VEGF and immunofluorescence staining of CD31 in different treatment groups at 7 d. Data are expressed as mean ± SD (n = 3). ***$P < 0.001$, **$P < 0.01$.

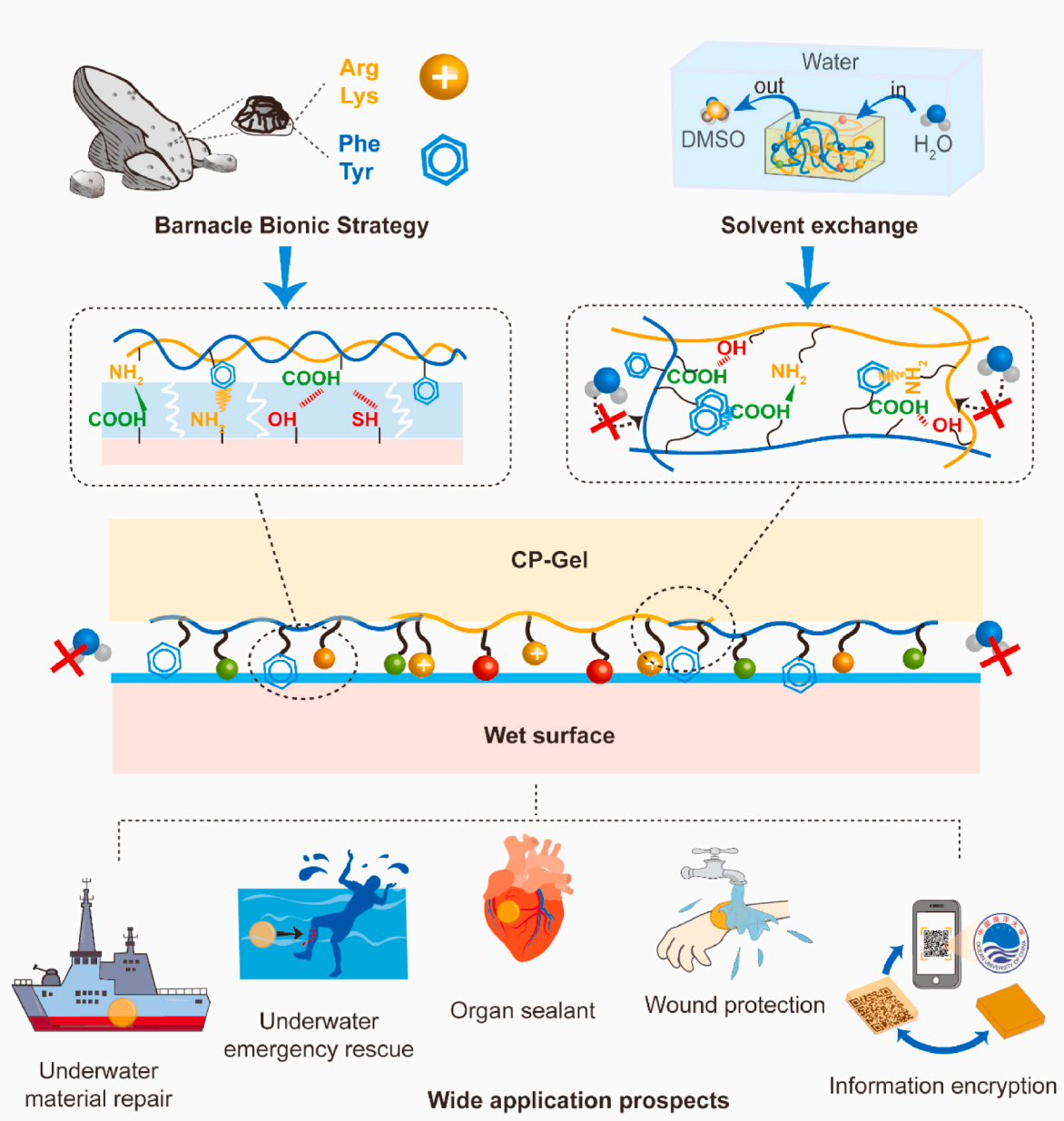

Fig. 9. Adhesion mechanism and application prospects of CP-Gel. The adverse effect of hydration layer on wet adhesion was reduced by mimicking BC. A double-crosslinking network was constructed by solvent exchange to reduce the effect of swelling on wet adhesion. The breaking of the hydration layer and controlling of swelling achieved robust wet adhesion of hydrogels. CP-Gel is expected to be used for underwater leak sealing, marine emergency rescue, organ sealant, daily care of water-contact wounds, and information encryption.

fluorescence intensity comparable to that of the control group (Fig. 7D). The results of hemolysis experiments showed that the Gel, C-Gel, P-Gel, and CP-Gel had approximately zero hemolysis effect; all hemolysis rates were less than 2 % (Fig. 7E), and there were no lesions or abnormalities in the heart, liver, spleen, lung, and kidney of rats treated with CP-Gel *in vivo* (Fig. 7F), indicating that they had good blood and organ compatibility, and thus, can be used as safe materials in the biomedical field [1,60,61].

3.7. Wound healing in seawater-immersed model

We constructed a seawater-immersed wound model to evaluate the ability of CP-Gel to promote wound healing (Fig. 8A). The healing rates of seawater-immersed wounds in SD rats at 3, 7, 10, and 14 d are shown in Fig. 8B–C. Compared with the control group, the hypertonic and alkaline environment of seawater aggravated wounds, resulting in edema, bleeding, and slower wound healing [10]. In contrast, CP-Gel significantly promoted seawater-immersed wound healing, with a wound healing rate of 97.66 ± 1.10 % at 14 d, better than that of the commercially available hydrogel-treated group (87.69 ± 0.13 %). In addition, the CP-Gel-treated group showed less inflammatory reactions, more neoplastic follicles and granulation tissue in H&E staining, and more collagen deposition in Masson staining at 7 d and 14 d (Fig. 8D).

In addition, to further verify the inflammation degrees and angiogenesis of wound tissue, the immunohistochemistry of Interleukin-6 (IL-6), tumor necrosis factor-α (TNF-α), ascular endothelial growth factor (VEGF) and immunofluorescence staining of platelet endothelial cell adhesion molecule-1 (CD31) were performed on rat wounds at 7 d (Fig. 8E). CP-Gel-treated group exhibited less expression of IL-6 and TNF-α and more expression of VEGF and CD31 fluorescence, indicating

that the CP-Gel-treated group reduced inflammatory response and promoted angiogenesis [2]. These results indicate that CP-Gel significantly promotes seawater-immersed wound healing, and has promising prospects for marine emergency care and water-contact wound protection.

3.8. Discussion and prospects

Compared to wet adhesive hydrogels reported in previous studies, the advantages of CP-Gel are as follows:

(1) Currently, research on barnacle-inspired materials focuses only on the amino acid composition [1,62] or advanced structure of proteins [24] in BC, ignoring the important roles of polysaccharides, especially chitin, which play a crucial role in the adhesion function of barnacle [21–23]. CP-Gel provides a novel idea for the development of wet adhesive hydrogels.
(2) CP-Gel combined with solvent exchange with barnacles is a new strategy to effectively improve the anti-swelling properties and adhesion of hydrogels [7,24]. More importantly, non-reactants can be effectively removed through solvent exchange, thus avoiding the toxicity and irritation of non-cross-linked monomers in other barnacle-inspired studies [17,63]. In addition, compared to mussel-inspired hydrogels, the potential toxicity and complex oxidative control of dopamine can be avoided [2,64].
(3) CP-Gel has various functions, which can be used not only for acute wounds with bleeding, chronic wounds with fluid exudation, and underwater wound care, but also is expected to be used for organ sealing, material leakage, controlled adhesion grasping hand, and information encryption. Compared to traditional adhesive materials [1,62], CP-Gel enables on-demand peeling to avoid pain and secondary injuries when changing dressings (Fig. 9).
(4) Compared to excessively increasing the crosslink density to resist swelling, our solvent exchange strategy formed a homogeneous double crosslink network to ensure the flexibility and extensibility of the hydrogels, which is helpful for improving wet adhesion.

However, our study also has some limitations. For example, the solvent exchange process requires a long preparation cycle, and the adhesion strength of our strategy needs to be further improved compared with the adhesion based on conventional organsilanes and catechols.

4. Conclusions

CP-Gel with robust wet adhesion and good biosafety was constructed using a barnacle-inspired strategy combined with solvent exchange. CTS and PEA reduced the adverse effects of the hydration layer on wet adhesion, while the solvent exchange strategy significantly improved the swelling resistance and structural stability of the hydrogels by forming a dynamic physical covalent double network. As a result, CP-Gel not only adhered firmly to various tissues and objects, but also exhibited strong adhesion in underwater environments and moving interfaces. On-demand detachment and controllable adhesion of CP-Gel were achieved by promoting swelling using an alkaline buffer solution. Benefiting from the strong wet adhesion properties of CP-Gel, it provides excellent protection and healing promotion for seawater-soaked wounds. In summary, our strategy of combining marine barnacle biomimetic with solvent exchange provides a novel and feasible method to enhance the wet adhesion of hydrogels, and shows significant potential for application.

Data availability

The data that support the findings of this study are available from the corresponding author upon reasonable request.

Ethics approval and consent to participant

The animal experiments were approved by the Ethics and Animal Welfare Committee of the Ocean University of China (OUC-SMP-2023-04-11).

The research described in this paper doesn't include human research participants.

CRediT authorship contribution statement

Guiyuan Zhao: Writing – original draft, Methodology, Investigation, Data curation. **Aijia Zhang:** Writing – original draft, Methodology, Investigation. **Xiangyan Chen:** Writing – original draft, Methodology. **Guangli Xiang:** Software, Investigation. **Tianze Jiang:** Supervision, Funding acquisition. **Xia Zhao:** Writing – review & editing, Writing – original draft, Supervision, Funding acquisition, Conceptualization.

Declaration of competing interest

The authors declare that they have no known competing financial interests or personal relationships that could have appeared to influence the work reported in this paper.

Acknowledgments

This work was supported by the National Natural Science Foundation of China (U21A20297) and Natural Science Foundation of Qingdao (202406).

Appendix A. Supplementary data

Supplementary data to this article can be found online at https://doi.org/10.1016/j.bioactmat.2024.07.011.

References

[1] Z. Ni, H. Yu, L. Wang, X. Liu, D. Shen, X. Chen, J. Liu, N. Wang, Y. Huang, Y. Sheng, Polyphosphazene and non-catechol-based antibacterial injectable hydrogel for adhesion of wet tissues as wound dressing, Adv. Healthcare Mater. 11 (1) (2022) e2101421, https://doi.org/10.1002/adhm.202101421.
[2] M. Zhang, Q. Zhang, X. Chen, T. Jiang, P. Song, B. Wang, X. Zhao, Mussel-inspired nanocomposite hydrogel based on alginate and antimicrobial peptide for infected wound repair, Int. J. Biol. Macromol. 219 (2022) 1087–1099, https://doi.org/10.1016/j.ijbiomac.2022.08.165.
[3] J. Xing, Y. Ding, X. Zheng, P. Yu, M. Qin, R. Qiu, Y. Li, S. Shang, J. Xie, J. Li, Barnacle-Inspired robust and aesthetic Janus patch with instinctive wet adhesive for oral ulcer treatment, Chem. Eng. J. 444 (2022) 136580, https://doi.org/10.1016/j.cej.2022.136580.
[4] H. Liu, S. Qin, J. Liu, C. Zhou, Y. Zhu, Y. Yuan, D.a. Fu, Q. Lv, Y. Song, M. Zou, Z. Wang, L. Wang, Bio-inspired self-hydrophobized sericin adhesive with tough underwater adhesion enables wound healing and fluid leakage sealing, Adv. Funct. Mater. 32 (32) (2022) 2201108, https://doi.org/10.1002/adfm.202201108.
[5] C. Xie, Y. Li, X. Guo, Y. Ding, X. Lu, S. Rao, Mussel-inspired adhesive hydrogels for local immunomodulation, Mater. Chem. Front. 7 (5) (2023) 846–872, https://doi.org/10.1039/d2qm01232d.
[6] Y. Lu, X. Huang, L. Yuting, R. Zhu, M. Zheng, J. Yang, S. Bai, Silk fibroin-based tough hydrogels with strong underwater adhesion for fast hemostasis and wound sealing, Biomacromolecules 24 (1) (2022) 319–331, https://doi.org/10.1021/acs.biomac.2c01157.
[7] G. Pan, F. Li, S. He, W. Li, Q. Wu, J. He, R. Ruan, Z. Xiao, J. Zhang, H. Yang, Mussel- and barnacle cement proteins-inspired dual-bionic bioadhesive with repeatable wet-tissue adhesion, multimodal self-healing, and antibacterial capability for nonpressing hemostasis and promoted wound healing, Adv. Funct. Mater. 32 (25) (2022) 2200908, https://doi.org/10.1002/adfm.202200908.
[8] X. Ma, X. Zhou, J. Ding, B. Huang, P. Wang, Y. Zhao, Q. Mu, S. Zhang, C. Ren, W. Xu, Hydrogels for underwater adhesion: adhesion mechanism, design strategies and applications, J. Mater. Chem. A 10 (22) (2022) 11823–11853, https://doi.org/10.1039/d2ta01960d.
[9] M. Amjadi, K.-U. Kyung, I. Park, M. Sitti, Stretchable, skin-mountable, and wearable strain sensors and their potential applications: a review, Adv. Funct. Mater. 26 (11) (2016) 1678–1698, https://doi.org/10.1002/adfm.201504755.

[10] Q. Fang, Z. Yao, L. Feng, T. Liu, S. Wei, P. Xu, R. Guo, B. Cheng, X. Wang, Antibiotic-loaded chitosan-gelatin scaffolds for infected seawater immersion wound healing, Int. J. Biol. Macromol. 159 (2020) 1140–1155, https://doi.org/10.1016/j.ijbiomac.2020.05.126.
[11] Y. Lv, F. Cai, Y. He, L. Li, Y. Huang, J. Yang, Y. Zheng, X. Shi, Multi-crosslinked hydrogels with strong wet adhesion, self-healing, antibacterial property, reactive oxygen species scavenging activity, and on-demand removability for seawater-immersed wound healing, Acta Biomater. 159 (2023) 95–110, https://doi.org/10.1016/j.actbio.2023.01.045.
[12] X. Wang, Y. Guo, J. Li, M. You, Y. Yu, J. Yang, G. Qin, Q. Chen, Tough wet adhesion of hydrogen-bond-based hydrogel with on-demand debonding and efficient hemostasis, ACS Appl. Mater. Interfaces 14 (31) (2022) 36166–36177, https://doi.org/10.1021/acsami.2c10202.
[13] S. Wang, J. Liu, L. Wang, H. Cai, Q. Wang, W. Wang, J. Shao, X. Dong, Underwater adhesion and anti-swelling hydrogels, Advanced Materials Technologies 8 (6) (2022) 2201477, https://doi.org/10.1002/admt.202201477.
[14] C.W. Peak, J.J. Wilker, G. Schmidt, A review on tough and sticky hydrogels, Colloid Polym. Sci. 291 (9) (2013) 2031–2047, https://doi.org/10.1007/s00396-013-3021-y.
[15] W. Huang, S. Cheng, X. Wang, Y. Zhang, L. Chen, L. Zhang, Noncompressible hemostasis and bone regeneration induced by an absorbable bioadhesive self-healing hydrogel, Adv. Funct. Mater. 31 (22) (2021) 2009189, https://doi.org/10.1002/adfm.202009189.
[16] H. Zhu, G. Xu, Y. He, H. Mao, D. Kong, K. Luo, W. Tang, R. Liu, Z. Gu, A dual-bioinspired tissue adhesive based on peptide dendrimer with fast and strong wet adhesion, Adv. Healthcare Mater. 11 (15) (2022) 2200874, https://doi.org/10.1002/adhm.202200874.
[17] H. Yuk, J. Wu, T.L. Sarrafian, X. Mao, C.E. Varela, E.T. Roche, L.G. Griffiths, C. S. Nabzdyk, X. Zhao, Rapid and coagulation-independent haemostatic sealing by a paste inspired by barnacle glue, Nat. Biomed. Eng. 5 (10) (2021) 1131–1142, https://doi.org/10.1038/s41551-021-00769-y.
[18] C. Liang, Z. Ye, B. Xue, L. Zeng, W. Wu, C. Zhong, Y. Cao, B. Hu, P.B. Messersmith, Self-assembled nanofibers for strong underwater adhesion: the trick of barnacles, ACS Appl. Mater. Interfaces 10 (30) (2018) 25017–25025, https://doi.org/10.1021/acsami.8b04752.
[19] C. Cui, C. Fan, Y. Wu, M. Xiao, T. Wu, D. Zhang, X. Chen, B. Liu, Z. Xu, B. Qu, W. Liu, Water-triggered hyperbranched polymer universal adhesives: from strong underwater adhesion to rapid sealing hemostasis, Adv. Mater. 31 (49) (2019) e1905761, https://doi.org/10.1002/adma.201905761.
[20] L. Han, M. Wang, L.O. Prieto-López, X. Deng, J. Cui, Self-hydrophobization in a dynamic hydrogel for creating nonspecific repeatable underwater adhesion, Adv. Funct. Mater. 30 (7) (2019) 1907064, https://doi.org/10.1002/adfm.201907064.
[21] H.-C. Lin, Y.H. Wong, C.-H. Sung, B.K.K. Chan, Histology and transcriptomic analyses of barnacles with different base materials and habitats shed lights on the duplication and chemical diversification of barnacle cement proteins, BMC Genom. 22 (1) (2021), https://doi.org/10.1186/s12864-021-08049-4.
[22] C. Liang, J. Strickland, Z. Ye, W. Wu, B. Hu, D. Rittschof, Biochemistry of barnacle adhesion: an updated review, Front. Mar. Sci. 6 (2019), https://doi.org/10.3389/fmars.2019.00565.
[23] M. Almeida, E.M. Fernandes, C.F. Marques, F.C.M. Lobo, R.O. Sousa, R.L. Reis, T. H. Silva, Structure and composition of the cuticle of the goose barnacle pollicipes pollicipes: a flexible composite biomaterial, Mar. Drugs 21 (2) (2023), https://doi.org/10.3390/md21020096.
[24] J. Huang, Y. Jiang, Y. Liu, Y. Ren, Z. Xu, Z. Li, Y. Zhao, X. Wu, J. Ren, Marine-inspired molecular mimicry generates a drug-free, but immunogenic hydrogel adhesive protecting surgical anastomosis, Bioact. Mater. 6 (3) (2021) 770–782, https://doi.org/10.1016/j.bioactmat.2020.09.010.
[25] C. Liang, X. Bi, K. Gan, J. Wu, G. He, B. Xue, Z. Ye, Y. Cao, B. Hu, Short peptides derived from a block copolymer-like barnacle cement protein self-assembled into diverse supramolecular structures, Biomacromolecules 23 (5) (2022) 2019–2030, https://doi.org/10.1021/acs.biomac.2c00031.
[26] Y. Zhan, W. Fu, Y. Xing, X. Ma, C. Chen, Advances in versatile anti-swelling polymer hydrogels, Mater. Sci. Eng., C 127 (2021) 112208, https://doi.org/10.1016/j.msec.2021.112208.
[27] J. Li, J. Ma, Q. Feng, E. Xie, Q. Meng, W. Shu, J. Wu, L. Bian, F. Han, B. Li, Building Osteogenic Microenvironments with a Double-Network Composite Hydrogel for Bone Repair, vol. 6, Research (Wash D C), 2023, p. 21, https://doi.org/10.34133/research.0021.
[28] X. Dou, H. Wang, F. Yang, H. Shen, X. Wang, D. Wu, One-step soaking strategy toward anti-swelling hydrogels with a stiff "armor", Adv. Sci. 10 (9) (2023) e2206242, https://doi.org/10.1002/advs.202206242.
[29] Y. Zong, L. Chen, X. Li, Q. Ding, W. Han, J. Lou, Highly robust and sensitive dual-network freeze-resistant organic hydrogel thermocells, Carbohydr. Polym. 314 (2023) 120958, https://doi.org/10.1016/j.carbpol.2023.120958.
[30] L. Xu, S. Gao, Q. Guo, C. Wang, Y. Qiao, D. Qiu, A solvent-exchange strategy to regulate noncovalent interactions for strong and antiswelling hydrogels, Adv. Mater. 32 (52) (2020) 2004579, https://doi.org/10.1002/adma.202004579.
[31] S. He, B. Guo, X. Sun, M. Shi, H. Zhang, F. Yao, H. Sun, J. Li, Bio-inspired instant underwater adhesive hydrogel sensors, ACS Appl. Mater. Interfaces 14 (40) (2022) 45869–45879, https://doi.org/10.1021/acsami.2c13371.
[32] Y. Wu, Y. Zhang, H. Wu, J. Wen, S. Zhang, W. Xing, H. Zhang, H. Xue, J. Gao, Y. Mai, Solvent-exchange-assisted wet annealing: a new strategy for superstrong, tough, stretchable, and anti-fatigue hydrogels, Adv. Mater. 35 (15) (2023) e2210624, https://doi.org/10.1002/adma.202210624.
[33] H. Li, F. Wang, Core-shell chitosan microsphere with antimicrobial and vascularized functions for promoting skin wound healing, Mater. Des. 204 (2021), https://doi.org/10.1016/j.matdes.2021.109683.
[34] A. Mohandas, S. Deepthi, R. Biswas, R. Jayakumar, Chitosan based metallic nanocomposite scaffolds as antimicrobial wound dressings, Bioact. Mater. 3 (3) (2018) 267–277, https://doi.org/10.1016/j.bioactmat.2017.11.003.
[35] S. Cao, G. Xu, Q. Li, S. Zhang, Y. Yang, J. Chen, Double crosslinking chitosan sponge with antibacterial and hemostatic properties for accelerating wound repair, Compos. B Eng. 234 (2022) 109746, https://doi.org/10.1016/j.compositesb.2022.109746.
[36] X.T. Cao, S. Kumar, I. Nemec, J. Kopp, R.S. Varma, Solvent-directed morphological transformation in covalent organic polymers, Frontiers in Materials 9 (2022), https://doi.org/10.3389/fmats.2022.889679.
[37] M. Wu, X. Chen, J. Xu, H. Zhang, Freeze-thaw and solvent-exchange strategy to generate physically cross-linked organogels and hydrogels of curdlan with tunable mechanical properties, Carbohydr. Polym. 278 (2022) 119003, https://doi.org/10.1016/j.carbpol.2021.119003.
[38] J. Yu, R. Xie, M. Zhang, K. Shen, Y. Yang, X. Zhao, X. Zhang, Y. Zhang, Y. Cheng, Molecular architecture regulation for the design of instant and robust underwater adhesives, Sci. Adv. 9 (22) (2023) eadg4031, https://doi.org/10.1126/sciadv.adg4031.
[39] X. Xu, V.V. Jerca, R. Hoogenboom, Bioinspired double network hydrogels: from covalent double network hydrogels via hybrid double network hydrogels to physical double network hydrogels, Mater. Horiz. 8 (4) (2021) 1173–1188, https://doi.org/10.1039/d0mh01514h.
[40] K. Lei, M. Chen, X. Wang, J. Gao, J. Zhang, G. Li, J. Bao, Z. Li, J. Li, Highly stretchable, self-healing elastomer hydrogel with universal adhesion driven by reversible cross-links and protein enhancement, J. Mater. Chem. B 10 (44) (2022) 9188–9201, https://doi.org/10.1039/d2tb02015g.
[41] H. Xu, Y. Tan, W. Rao, D. Wang, S. Xu, W. Liao, Y.Z. Wang, Ultra-strong mechanical property and force-driven malleability of water-poor hydrogels, J. Colloid Interface Sci. 542 (2019) 281–288, https://doi.org/10.1016/j.jcis.2019.02.015.
[42] Y. Zhang, X. Zhu, B. Chen, Adhesion force evolution of protein on the surfaces with varied hydration extent: quantitative determination via atomic force microscopy, J. Colloid Interface Sci. 608 (Pt 1) (2022) 255–264, https://doi.org/10.1016/j.jcis.2021.09.131.
[43] D. Victoria-Valenzuela, A.B. Morales-Cepeda, E.I. Cárdenas-Rangel, Toward an understanding of the effects of nanocellulose during the free-radical polymerization reactions. Kinetic aspects of suspension-free radical polymerization of methyl methacrylate (MMA) in the presence and absence of nanocellulose, J. Polym. Res. 30 (6) (2023), https://doi.org/10.1007/s10965-023-03637-2.
[44] X. Liu, Q. Zhang, G. Gao, Solvent-Resistant and nonswellable hydrogel conductor toward mechanical perception in diverse liquid media, ACS Nano 14 (10) (2020) 13709–13717, https://doi.org/10.1021/acsnano.0c05932.
[45] M. Li, H. Lu, M. Pi, H. Zhou, Y. Wang, B. Yan, W. Cui, R. Ran, Water-induced phase separation for anti-swelling hydrogel adhesives in underwater soft electronics, Adv. Sci. 10 (32) (2023) e2304780, https://doi.org/10.1002/advs.202304780.
[46] H. Guo, S. Huang, A. Xu, W. Xue, Injectable adhesive self-healing multiple-dynamic-bond crosslinked hydrogel with photothermal antibacterial activity for infected wound healing, Chem. Mater. 34 (6) (2022) 2655–2671, https://doi.org/10.1021/acs.chemmater.1c03944.
[47] Y. Zhou, L. Jin, Mechanics underpinning phase separation of hydrogels, Macromolecules 56 (2) (2023) 426–439, https://doi.org/10.1021/acs.macromol.2c02356.
[48] H. Wang, X. Su, Z. Chai, Z. Tian, W. Xie, Y. Wang, Z. Wan, M. Deng, Z. Yuan, J. Huang, A hydra tentacle-inspired hydrogel with underwater ultra-stretchability for adhering adipose surfaces, Chem. Eng. J. 428 (2022) 131049–131057, https://doi.org/10.1016/j.cej.2021.131049.
[49] X. Liu, Q. Zhang, L. Duan, G. Gao, Bioinspired nucleobase-driven nonswellable adhesive and tough gel with excellent underwater adhesion, ACS Appl. Mater. Interfaces 11 (6) (2019) 6644–6651, https://doi.org/10.1021/acsami.8b21686.
[50] Y. Wu, W. Xing, J. Wen, Z. Wu, Y. Zhang, H. Zhang, H. Wu, H. Yao, H. Xue, J. Gao, Mixed solvent exchange enabled high-performance polymeric gels, Polymer 267 (2023), https://doi.org/10.1016/j.polymer.2022.125661.
[51] M. Li, H. Lu, X. Wang, Z. Wang, M. Pi, W. Cui, R. Ran, Regulable mixed-solvent-induced phase separation in hydrogels for information encryption, Small 18 (52) (2022) e2205359, https://doi.org/10.1002/smll.202205359.
[52] X. Du, Y. Hou, L. Wu, S. Li, A. Yu, D. Kong, L. Wang, G. Niu, An anti-infective hydrogel adhesive with non-swelling and robust mechanical properties for sutureless wound closure, J. Mater. Chem. B 8 (26) (2020) 5682–5693, https://doi.org/10.1039/d0tb00640h.
[53] Y. Jiang, X. Zhang, W. Zhang, M. Wang, L. Yan, K. Wang, L. Han, X. Lu, Infant skin friendly adhesive hydrogel patch activated at body temperature for bioelectronics securing and diabetic wound healing, ACS Nano 16 (6) (2022) 8662–8676, https://doi.org/10.1021/acsnano.2c00662.
[54] M. Lee, Y.S. Kim, J. Park, G. Choe, S. Lee, B.G. Kang, J.H. Jun, Y. Shin, M. Kim, Y. Ahn, J.Y. Lee, A paintable and adhesive hydrogel cardiac patch with sustained release of ANGPTL4 for infarcted heart repair, Bioact. Mater. 31 (2024) 395–407, https://doi.org/10.1016/j.bioactmat.2023.08.020.
[55] H. Wang, X. Yi, T. Liu, J. Liu, Q. Wu, Y. Ding, Z. Liu, Q. Wang, An integrally formed janus hydrogel for robust wet-tissue adhesive and anti-postoperative adhesion, Adv. Mater. 35 (23) (2023), https://doi.org/10.1002/adma.202300394.
[56] C. Cai, H. Zhu, Y. Chen, Y. Guo, Z. Yang, H. Li, H. Liu, Mechanoactive nanocomposite hydrogel to accelerate wound repair in movable parts, ACS Nano 16 (12) (2022) 20044–20056, https://doi.org/10.1021/acsnano.2c07483.

[57] S.M.F. Kabir, P.P. Sikdar, B. Haque, M.A.R. Bhuiyan, A. Ali, M.N. Islam, Cellulose-based hydrogel materials: chemistry, properties and their prospective applications, Prog Biomater 7 (3) (2018) 153–174, https://doi.org/10.1007/s40204-018-0095-0.

[58] Y.W. Lee, S. Chun, D. Son, X. Hu, M. Schneider, M. Sitti, A tissue adhesion-controllable and biocompatible small-scale hydrogel adhesive robot, Adv. Mater. 34 (13) (2022) e2109325, https://doi.org/10.1002/adma.202109325.

[59] A. Eklund, O. Ikkala, H. Zhang, Highly efficient switchable underwater adhesion in channeled hydrogel networks, Adv. Funct. Mater. (2023), https://doi.org/10.1002/adfm.202214091.

[60] S. Li, Y. Xian, G. He, L. Chen, Z. Chen, Y. Hong, C. Zhang, D. Wu, In situ injectable tetra-PEG hydrogel bioadhesive for sutureless repair of gastrointestinal perforation, Chin. J. Chem. 41 (23) (2023) 3339–3348, https://doi.org/10.1002/cjoc.202300312.

[61] Y. Dong, Y. Li, B. Fan, W. Peng, W. Qian, X. Ji, D. Gan, P. Liu, Long-term antibacterial, antioxidative, and bioadhesive hydrogel wound dressing for infected wound healing applications, Biomater. Sci. 11 (6) (2023) 2080–2090, https://doi.org/10.1039/d2bm01981g.

[62] H. Fan, J. Wang, J.P. Gong, Barnacle cement proteins-inspired tough hydrogels with robust, long-lasting, and repeatable underwater adhesion, Adv. Funct. Mater. 31 (11) (2020) 2009334, https://doi.org/10.1002/adfm.202009334.

[63] D. Hao, X. Li, E. Yang, Y. Tian, L. Jiang, Barnacle inspired high-strength hydrogel for adhesive, Front. Bioeng. Biotechnol. 11 (2023) 1183799, https://doi.org/10.3389/fbioe.2023.1183799.

[64] J. Chen, L. Han, J. Liu, H. Zeng, Mussel-inspired adhesive hydrogels: chemistry and biomedical applications, Chin. J. Chem. 41 (24) (2023) 3729–3738, https://doi.org/10.1002/cjoc.202300423.